Subsection G
Other RGS Proteins

[22] Identification and Functional Analysis of Dual-Specific A Kinase-Anchoring Protein-2

By L. L. BURNS-HAMURO, D. M. BARRACLOUGH, and S. S. TAYLOR

Abstract

Since the cloning of dual-specificity A kinase-anchoring protein 2 (D-AKAP2), there has been considerable progress in understanding the structural features of this AKAP and its interaction with protein kinase A (PKA). The domain organization of D-AKAP2 is quite unique, containing two tandem, putative RGS domains, a PKA-binding motif, and a PDZ (PSD95/Dlg/ZO1)-binding motif. Although the function of D-AKAP2 has remained elusive, several reports suggest that D-AKAP2 is targeted to cotransporters in the kidney and that it may play a role in regulating transporter activity. In addition, the finding that a single nucleotide polymorphism in the PKA-binding region of D-AKAP2 may contribute to increased morbidity and mortality emphasizes the potential importance of this protein in pathogenesis. The first part of this article focuses on initial efforts to identify and clone D-AKAP2, followed by tissue localization and expression profiles. The latter half of the article focuses on the domain organization of D-AKAP2 and its interaction with PKA. Finally, a comprehensive analysis of the PKA binding motif is described, which has led to the development of novel peptides derived from D-AKAP2 that can be useful tools in probing the function of this AKAP in cellular and animal models.

Introduction

Dual-specific A kinase-anchoring protein 2 (D-AKAP2) is unique among mammalian regulator of G-protein signaling (RGS) proteins in that it contains two RGS domains and a protein kinase A (PKA)-binding motif (Fig. 1A). It was initially identified in a yeast two hybrid assay designed to screen for interacting proteins of the type I regulatory subunit (RI) of protein kinase A (Huang *et al.*, 1997a). The C-terminal 40 residues of the protein identified in the screen interacted specifically and with high affinity to three of the four regulatory subunit isoforms of PKA, defining it as a

0076-6879/04 $35.00

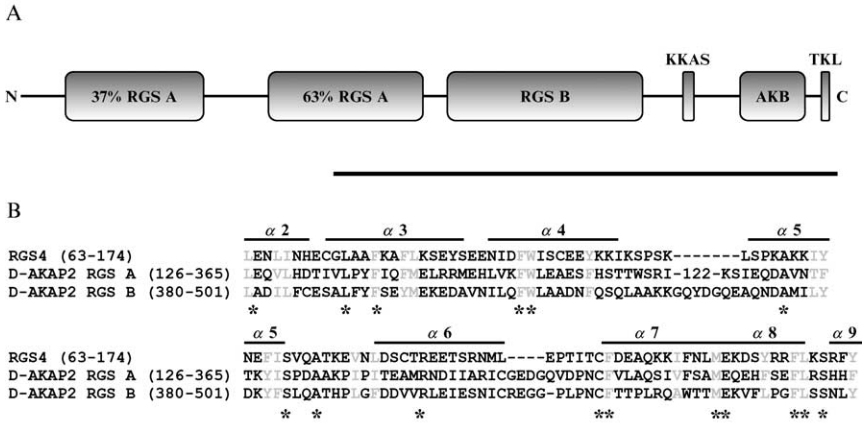

FIG. 1. (A) Domain organization of human D-AKAP2. RGS, regulator of G-protein signaling domain; KKAS, phosphorylation consensus site for PKA; AKB, A kinase-binding domain; TKL, PDZ-binding motif. (B) Sequence alignment of the two RGS domains of D-AKAP2 (RGS A and RGS B) with RGS4 using Clustal W alignment software. The asterisk (*) denotes identical residues, and residues in gray denote conserved hydrophobic residues observed for this fold (Tesmer *et al.*, 1997). Reprinted from Hamuro *et al.* (2002), with permission.

"dual-specific" A kinase-anchoring protein (D-AKAP). Subsequent cloning of mouse and human genes revealed two regions of unmistakable homology to RGS domains (Hamuro *et al.*, 2002a; Huang *et al.*, 1997a; Wang *et al.*, 2001) (Fig. 1B).

In general, AKAPs act as scaffold proteins, coordinating the activity of PKA by binding and localizing PKA and other signaling proteins to form localized transduction units, which serve to regulate the activity of the kinase and to increase the fidelity of receptor-specific cAMP-mediated signaling (Colledge and Scott, 1999; Edwards and Scott, 2000). As a scaffold protein, D-AKAP2 has the potential to coordinate a signaling complex that links cAMP signaling with G-protein-coupled receptor (GPCR) signaling. Although there have been no Gα-binding partners identified for D-AKAP2, there are some interesting leads as to the functional implications of this protein.

D-AKAP2 has been linked indirectly to a Na^+-dependent phosphate cotransporter (NaPi-IIa) in the brush border of the kidney via its interaction with PDZ proteins, PDZK1 and NHERF-1 (Gisler *et al.*, 2003a,b). Both PDZK1 and NHERF-1 contain multiple PDZ domains and interact directly with the C terminus of NaPi-IIa (Gisler *et al.*, 2001; Hernando *et al.*, 2002). PDZK1 contains four tandem PDZ domains and is a major

component in the brush border cells of the kidney (Gisler *et al*., 2003a,b). The third PDZ domain of PDZK1 binds to the NaPi-IIa cotransporter, while the fourth domain binds to the C-terminal PDZ-binding motif of D-AKAP2 (Gisler *et al*., 2003a). NaPi-IIa is primarily responsible for inorganic phosphate reabsorption in the proximal tubule of the kidney, which is regulated by diet and the parathyroid hormone (PTH) (Murer *et al*., 2003). Regulated endocytosis of the cotransporter is mediated by PTH and involves a network of protein kinases, which is believed to be responsible for regulating the level of the receptor at the brush border membrane (Bacic *et al*., 2003; Murer *et al*., 2003). Interestingly, NHERF-1 also interacts with the Na^+/H^+ exchanger (NHE-3) and recruits PKA via the ezrin AKAP to downregulate channel activity (Weinman *et al*., 2000, 2001). The detailed mechanism of D-AKAP2-mediated PKA regulation of the NaPi-IIa cotransporter is not known. However, the implication is that D-AKAP2 is recruiting PKA to NaPi-IIa indirectly through the PDZ proteins and is potentially involved in regulating the level of the cotransporter at the membrane by receptor endocytosis and/or vesicular trafficking (Gisler *et al*., 2003a).

In addition to the association of D-AKAP2 with cotransporters in the kidney, genomic efforts have identified several, single nucleotide polymorphisms (SNPs) associated with the human D-AKAP2 gene, two of which are located in exons and code for amino acid sequence changes in the protein (Kammerer *et al*., 2003). One of the SNPs is located in the N-terminal RGS domain of D-AKAP2 and codes for an arginine-to-histidine change at position 249 (R249H). The functional consequences of this residue change are not known, as no interacting G proteins have been identified. The other coding SNP is located in the PKA-binding region of the protein and codes for an amino acid change at position 646 (I646V). This sequence change alters binding to only the type I regulatory subunit ($RI\alpha$) of PKA. In a search for SNPs associated with morbidity and mortality, it was found that an older population of healthy volunteers had a reduced frequency of Val at position 646 compared with a younger population. This suggests that this particular sequence change, which enhances the affinity of PKA by a factor of three, increases the mortality and/or morbidity of the aging population, removing this segment from the healthy donating pool. Although a particular disease has not been associated with the SNP, preliminary evidence suggests an association with cardiac pathology. Patients that are homozygous for the valine allele (Val/Val) have statistically distinct parameters on echocardiogram measurements (Kammerer *et al*., 2003). Although this is not a direct indication of a disease process, this finding underscores the potential importance of this protein and continued efforts are underway to investigate the biology of D-AKAP2 further.

The first half of this article begins by describing (1) the identification of D-AKAP2 using a yeast two hybrid screen, (2) cloning and characterization of mouse and human proteins, (3) *in Vitro* and *in vivo* association of the protein with PKA, and (4) protein expression levels in mouse tissue and evidence for mitochondrial localization. The second half of the article presents a detailed characterization of the domain structure of this protein, including a model of the RGS domain of D-AKAP2, and describes how we have been able to optimize the selectivity of the R-binding motif of D-AKAP2 using peptide arrays. This has enabled the design of isoform-selective peptide disruptors of AKAP-mediated PKA localization that can be used to elucidate the function of this dual-specificity AKAP in cell and animal studies.

Identification and Cloning of D-AKAP2

D-AKAP2 was initially identified in a yeast two hybrid screen using Ret/ptc2 as the bait (Huang *et al*., 1997a). Ret/ptc2 is an oncoprotein with the C-terminal domain of the Ret receptor tyrosine kinase fused to the N terminus of the RIα subunit of PKA that contains the dimerization/docking (D/D) domain and is critical for AKAP binding. After screening a mouse embryonic cDNA library, several interacting clones were identified, eight of which coded for novel protein fragments designated R potential binding protein (RPP): RPP7, RPP8, and RPP9. Both RPP7 and RPP8 were identified as novel binding proteins of PKA and were characterized further. RPP7 was identified as D-AKAP1 and characterization of this protein can be found elsewhere (Huang *et al*., 1997b, 1999; Ma and Taylor, 2002).

To obtain the full-length clone of RPP8, an adult mouse testis cDNA library expressed in λgt10 was screened using ^{32}P-labeled RPP8 cDNA as described in Huang *et al*. (1997a). Positive phage cDNAs were isolated and cloned into pBluescript KS(+). The cDNAs were sequenced and used to search the BLAST database at the National Library of Medicine, National Institutes of Health. From the mouse testis cDNA library, the full-length cloned appeared to code for a 372 amino acid protein (Fig. 1A, black bar). The cDNA contained a stop codon just upstream of what was believed at the time to be the initiator methionine, followed by a stop codon and a poly(A) tail. There was no overall nucleotide sequence homology to known proteins when the sequence was compared with sequences from the GenBank database. However, amino acid residues 70–125 showed homology to RGS domains from several RGS proteins.

After the cloning of mouse D-AKAP2, it became apparent from western blots of mouse tissue extracts using several polyclonal antibodies

directed against different regions of the protein that at least some expressed protein contained a higher apparent molecular mass than the coding sequence predicted. Estimates from the western blot were 70–100 kDa, whereas the molecular mass of the coding sequence was ~43 kDa. Verification of a larger D-AKAP2 gene came from Fisher and Chatterjee when they submitted the gene sequence for human D-AKAP2 (GenBank ID AF037439) to the National Center for Biotechnology Information (NCBI), which suggested a larger coding region. To help resolve this discrepancy, human D-AKAP2 was cloned.

Human D-AKAP2 was cloned from a human brain cDNA library (Clontech) using 5′ and 3′ primers to the coding region of the human gene as described in Wang *et al.* (2001). After amplifying the cDNA by polymerase chain reaction (PCR), a 2.5-kb insert was ligated into a plasmid (pSP73) and sequenced. The cDNA of human D-AKAP2 codes for a 74-kDa, 662 amino acid protein. Using the BLAST human genome database, the gene was localized to chromosome 17q and contained 15 exons. The previously cloned mouse gene, which coded for 372 amino acids, was 94% identical to the C terminus of the human protein. This region included the C-terminal RGS domain and the PKA-binding site. A longer mouse sequence for D-AKAP2 (GenBank ID AK049399) has been submitted to GenBank by the Fantom Consortium and the Riken Genome Exploration Research Group (Okazaki *et al.*, 2002). This sequence was identified from a 7-day mouse embryonic, whole body cDNA library and codes for a 662 amino acid protein that is 93% identical to human D-AKAP2, verifying that cDNAs for both mouse and human code for identical length, highly homologous proteins. However, protein expression patterns from mouse tissue suggest that alternative length proteins can be expressed in a tissue-specific manner, as described later.

D-AKAP2 Interacts with Regulatory Subunit Isoforms of PKA

The interaction of D-AKAP2 with PKA was initially verified by expressing the C-terminal 40 residues of D-AKAP2 (RPP8) as a GST fusion protein using the plasmid pGEX-KG as described in Huang *et al.* (1997a). The RPP8 fusion protein, designated GST-RPP8, is expressed in *Escherichia coli* BL21(DE3). Bacteria are grown at 37° for approximately 8 h until an optical density of 0.8 absorbance units at 600 nm is reached. After lowering the temperature to 24°, protein expression is induced with 0.5 m*M* isopropyl β-D-thiogalactoside for 10–12 h. The cell pellet is frozen at −20°. Cell pellets are lysed by sonication in PBS (10 m*M* potassium phosphate, 150 m*M* NaCl, pH 7.4) with 0.1% Triton X-100, 1 m*M* EDTA, 5 m*M* 2-mercaptoethanol, and the protease inhibitors 1 m*M* phenylmethylsulfonyl fluoride and 5 m*M*

benzamidine. After centrifugation, the soluble fraction containing GST-RPP8 is incubated with glutathione resin for 2 h at 4°. Resin-bound GST-RPP8 is rinsed extensively with the same buffer used for cell lysis, and 100–200 μg of purified PKA regulatory subunit (RIα, RIβ, RIIα, or RIIβ) is added and incubated for 2 h at 4°. After extensive washing of the resin with PBS, the bound regulatory subunit is eluted by boiling in SDS gel-loading buffer and is analyzed by SDS–PAGE. Three of the four regulatory subunit isoforms of PKA (RIα, RIIα, and RIIβ) interact specifically with GST-RPP8 and not with a GST alone control (Huang *et al.*, 1997a).

Making use of the fact that the regulatory subunits of PKA bind cAMP with high affinity, *in vivo* association of D-AKAP2 with regulatory subunit isoforms of PKA in mouse brain extracts was investigated using a cAMP resin (Wang *et al.*, 2001). Mouse brain extracts are prepared by homogenizing the tissue in cold homogenization buffer [20 m*M* HEPES, pH 7.4, 20 m*M* NaCl, 5 m*M* EDTA, 5 m*M* EGTA, 0.5% Triton X-100, 1 m*M* dithiothreitol (DTT)] and a protease inhibitor cocktail (Calbiochem). After centrifuging at 10,000*g* for 30 min, the supernatants are incubated with cAMP agarose (Sigma) overnight. As a negative control, a similar incubation is carried out in the presence of 50 m*M* cAMP, which serves as a competitive inhibitor of regulatory subunit binding to the cAMP affinity resin. The resin is washed several times with a high salt wash buffer (10 m*M* HEPES, pH 7.4, 1.5 m*M* $MgCl_2$, 10 m*M* KCl, 0.5 M NaCl, 0.1% Nonidet P-40, 1 m*M* DTT, and protease inhibitors) and a low salt buffer (high salt buffer without NaCl). Any associated protein is eluted with 25 m*M* cAMP by rotating for 1 h at room temperature. The eluted protein is precipitated (10% TFA), and interacting proteins are detected by western blot using commercially available antibodies for RIα, RIIα (Transduction Laboratories, Lexington, KY), RIIβ (Biomol, Plymouth Meeting, PA), and anti-D-AKAP2. D-AKAP2 associates with both RIIα and RIIβ, but not RIα in this assay (Wang *et al.*, 2001). The inability to detect an interaction with RIα may be due to the reduced binding affinity to this isoform as described later, or to the fact that the RIα isoform is not detected at appreciable levels in brain extracts.

RNA and Protein Expression Levels of D-AKAP2 and Mitochondrial Localization

The mRNA and protein expression levels for D-AKAP2 are evaluated from various mouse tissues (Huang *et al.*, 1997a; Wang *et al.*, 2001). To investigate the tissue expression level of D-AKAP2 mRNA, Northern blots containing 2 μg of poly(A)$^+$ RNA from adult mouse tissues are

probed with ^{32}P-labeled RPP8 cDNA. A 5-kb mRNA is detected in all mouse tissues examined (Huang *et al*., 1997a). A weak 10-kb signal is detected in the brain, skeletal muscle, kidney, and testis. Furthermore, the testes contain additional smaller mRNA fragments of 3.4, 2.8, and 1.8 kb, suggesting alternative processing in the testes.

D-AKAP2 is expressed ubiquitously in mouse tissue. Western blots using polyclonal antibodies against D-AKAP2 reveal that the mouse tissue examined (white adipose tissue, brown adipose tissue, skeletal muscle, tongue, small intestine, kidney, lung, brain, pancreas, heart, spleen, and liver) express some level of the protein (Wang *et al*., 2001). The protein is most abundant in heart, brain, pancreas, and brown adipose tissue with variations in molecular weight seen throughout different tissues. For example, two prominent bands are detected in brain extracts that have very similar molecular weights. In addition, brown adipose tissue, skeletal muscle, small intestine, kidney, and heart all have high molecular weight and low molecular species, suggesting alternative mRNA splicing or degradation of the protein in these tissues (Wang *et al*., 2001). Gisler *et al*. (2003a) have cloned D-AKAP2 cDNA from a mouse kidney cDNA library and found that the cDNA coded a protein 372 amino acids, similar to the initial clone identified from an adult mouse testes library (Huang *et al*., 1997a). The molecular mass of endogenously expressed D-AKAP2 from adult mouse kidney was slightly larger than 40 kDa, consistent with the cDNA clone from kidney (Gisler *et al*., 2003a). Therefore, there appears to be heterogeneity in the length of the protein expressed in mouse and this heterogeneity seems to be tissue specific and suggestive of alternative splicing.

The cellular distribution of D-AKAP2 was evaluated using fractionated mouse brown adipose tissue and by staining intact cells (Wang *et al*., 2001). Mitochondria are isolated from cell lysates using centrifugation and a sucrose gradient. Homogenized brown adipose tissue in 250 m*M* sucrose is spun at 8500*g* to obtain the cytosolic fraction. The pellet is resuspended and recentrifuged at 800*g* to remove the nuclear pellet. The supernatant is centrifuged for an additional 8500*g* to obtain the mitochondrial pellet. The mitochondrial pellet is washed in 100 m*M* KCl with 1% bovine serum albumin (BSA) and the quality of the mitochondria is verified by electron microscopy (Wang *et al*., 2001). Aliquots from the cytosolic, nuclear, and mitochondrial fractions are resolved by SDS–PAGE and the protein is detected by a western blot. D-AKAP2 is found in the cytosolic, nuclear, and mitochondrial fractions from brown adipose tissue with a greater concentration in the mitochondria and nuclear fractions. Immunostaining of intact cells revealed that D-AKAP2 can associate with the mitochondria in addition to being cytoplasmic. Mitochondrial localization was observed in both a mouse cell line (C2 mouse myocytes) and primary rat cardiomyocytes

(Wang *et al.*, 2001). The low level of cytoplasmic and nuclear staining, in addition to the concentrated mitochondrial staining pattern for this protein, suggests that there may be multiple intracellular pools of D-AKAP2 in the cell. Immunohistochemistry and confocal microscopy of rat tissue revealed that at the neuromuscular junction, D-AKAP2 is rather diffuse as well and is present in both presynaptic and postsynaptic borders (Perkins *et al.*, 2001). Interestingly, in surrounding muscle, D-AKAP2 is present near the actin region and does not colocalize with mitochondria (Perkins *et al.*, 2001). This suggests that D-AKAP2 localization with the mitochondria is dependent on the cell type. This, in addition to the ubiquitous expression patterns, suggests that D-AKAP2 may have multiple cellular roles and/or is involved in a basal cellular function.

Defining the Domain Organization of D-AKAP2: Modeling the RGS Domain

AKAPs in general are large proteins that contain multiple recognition domains for many different interacting proteins. Several approaches were taken to delineate structural features of D-AKAP2. Initial sequence homology modeling revealed two regions of D-AKAP2 that contained homology to RGS domains. The domain boundaries of these RGS domains were defined further and a structural homology model of the C-terminal RGS domain was constructed using the known structure of RGS4 (Hamuro *et al.*, 2002a). In addition, the domain boundaries of the protein were evaluated using limited trypsin proteolysis and isotopic amide hydrogen exchange, which measures the exchange rate of backbone amide hydrogens in a protein (Hamuro *et al.*, 2002a).

Human D-AKAP2 was used to search the NCBI CDD database using RPS-BLAST. Two domains matching SMART 000315 and Pfam PF00615 were identified as RGS domains (Fig. 1A). The N-terminal RGS domain (RGS A) was split into two segments representing 37% (residues 125–168) and 63% (residues 292–368) of the domain. Interestingly, the split segments were separated by an ~122 amino acid insert that maps between helix 4 and 5 of the predicted RGS domain based on homology modeling to RGS4 (Fig. 1B). The C-terminal RGS domain (RGS B) includes residues 380–505. The presence of two RGS domains and the split nature of RGS A are features recognized to be present only in lower eukaryotic RGS domain-containing proteins (De Vries *et al.*, 2000). In a phylogenetic classification of RGS domain-containing proteins, the RGS B domain of D-AKAP2 was found to be distinct from other mammalian proteins (Zheng *et al.*, 1999). This may explain the inability to detect an interaction with traditional Gα proteins.

The PKA-binding site of D-AKAP2 [A kinase-binding (AKB) domain] is located at the C terminus of the protein (Fig. 1A). The AKB domain is characteristic of other AKAP proteins in that there are repeating units of hydrophobic (particularly branched chain residues) and hydrophillic residues, which form an amphipathic helical docking motif. This motif is described in detail in the next section. The last C-terminal residues of the protein contain a PDZ (PSD95/Dlg/ZO1)-binding motif. As described earlier, this motif has been implicated in tethering D-AKAP2 to a NaPi-IIa cotransporter in the brush border of the kidney via PDZ proteins (Gisler *et al*., 2003a).

A structural homology model of the RGS B domain of D-AKAP2 was constructed using the SwissModel server as described in Hamuro *et al*. (2002a). The X-ray structure coordinates for chain E of AlF_4^--activated $G_{i\alpha1}$ with RGS4 from rat (PDB ID: 1AGR_E) used as a template. RGS4 is a helical protein containing nine alpha helices connected by turns and loops (Tesmer *et al*., 1997). The amino acid sequence of RGS B was threaded onto the crystal structure of RGS4, including helices 2 through 9. Helix 1 did not show significant homology to RGS4 and was not used. Once the sequence was threaded onto the structure using the first approach mode of the SwissModel server, the final structural model was subjected to additional energy minimization using the GROMOS 43b1 force field as implemented in the DeepBlue SwissPDB viewer (Guex and Peitsch, 1997) using 5000 cycles of steepest descent followed by 5000 cycles of conjugate gradients. All computations were done *in vacuo*, without reaction field. Harmonic constraints of 50 C factors and 2500 C factors were used for each method. The final model was validated using the Biotech Validation Suite for Protein structures (http://biotech.ebi.ac.uk:8400). The aligned structures of RGS4 and the modeled RGS B domain of D-AKAP2 are shown in Fig. 2A. The alignment of the backbone α carbons of the RGS4 template and RGS B were within 0.7 Å with a *Z*-score of 6.0, indicating a high level of structural similarity.

In addition to sequence and structural homology modeling of D-AKAP2 to predict the domain organization of the protein, the folded regions of the protein were probed experimentally using hydrogen/deuterium exchange mass spectrometry (DXMS). Isotopic exchange of protein backbone amide hydrogens has been around for many decades, reviewed in Englander *et al*. (1997). The idea behind this approach is that if a protein is exposed to deuterium (^{2}H), labile hydrogens will exchange at some rate with the isotope, resulting in a heavy atom derivative at the site of exchange. The heavy atom can then be followed by nuclear magnetic resonance or mass spectrometry. Amide hydrogens from the protein backbone exchange with deuterium over a range of timescales that correlate with the

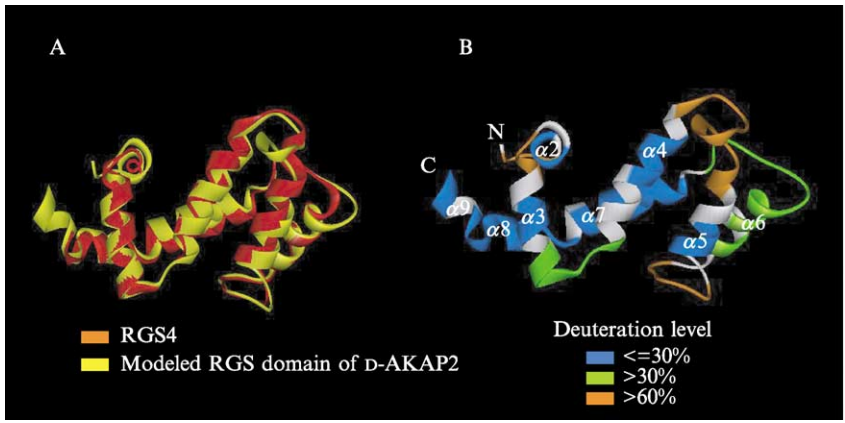

FIG. 2. (A) A backbone structural alignment of RGS4 and modeled RGS B domain of D-AKAP2. (B) Deuterium exchange data after 3000 s on exchange mapped onto the structure of the modeled RGS B domain. Reprinted from Hamuro *et al.* (2002), with permission.

degree of solvent exposure of the hydrogen and the structural context (i.e., hydrogen-bonding network) of the backbone amide hydrogen (Engen and Smith, 2001). This enables the technique to be used to map folded regions of proteins (Hamuro *et al.*, 2002b; Resing *et al.*, 1999; Yan *et al.*, 2002; Zhang and Smith, 1993), protein–protein interactions (Anand *et al.*, 2002; Ehring, 1999; Mandell *et al.*, 2001), and small ligand-binding sites (Andersen *et al.*, 2001; Engen *et al.*, 1999; Hamuro *et al.*, 2002c). An overview of this technique to evaluate the conformational properties of a protein is illustrated in Fig. 3. The protein is incubated in deuterated buffer for various lengths of time ranging from 10 s to several days. The deuterated protein is then quenched in acidic conditions to prevent back-exchange of the deuterium and the sample is cleaved with an acid-insensitive protease (pepsin), which cleaves the protein into numerous peptide fragments of varying lengths. The peptides are resolved over a C18 column in line with an electrospray mass spectrometry and the resulting mass of the peptides is determined. Peptides from regions of the protein that are highly solvent exposed will contain a greater number of deuterons (higher MW) than peptides from regions that are in solvent-inaccessible regions or folded regions of the protein. A detailed description of this technique can be found in other reviews (Engen and Smith, 2001; Englander *et al.*, 1997; Hamuro *et al.*, 2003; Hoofnagle *et al.*, 2003). The following is a summary of the technique used for the analysis of D-AKAP2 (Hamuro *et al.*, 2002b).

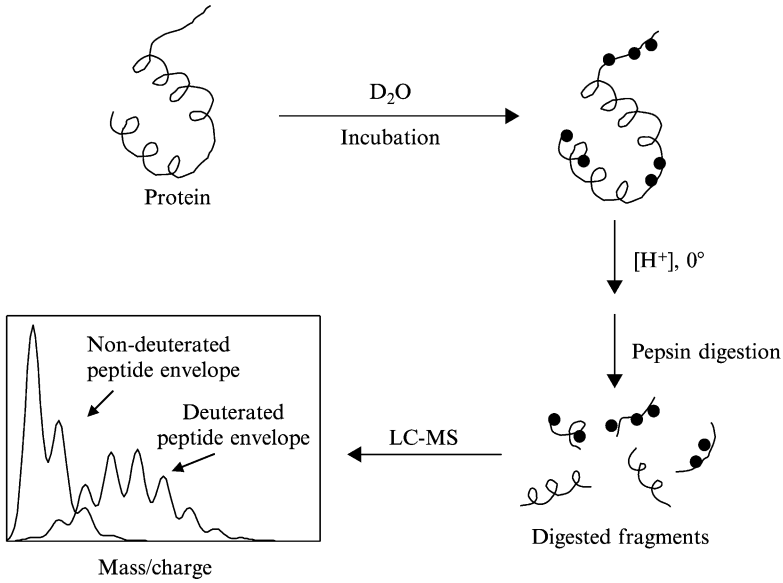

FIG. 3. Mapping the conformational properties of a protein using deuterium exchange mass spectrometry (DXMs). The protein is incubated in a deuterated buffer solution for various times ranging from 10 s to several days. To determine the location of the exchanged hydrogens, the protein is quenched under acidic conditions near 0° and is digested into numerous peptide fragments using an acid-insensitive protease (i.e., pepsin). The peptide fragments are separated by high-performance liquid chromatography (HPLC), and the extent of deuteration is determined by measuring the mass-to-charge ratio of each peptide isotopic envelope by mass spectrometry.

Full-length human D-AKAP2 (662 amino acids) is not expressed as a soluble protein in bacteria. We use a soluble form of mouse D-AKAP2 (375 amino acids), which includes the C-terminal half of RGS A, the full RGS B domain, the PKA-binding site, and the PDZ-binding motif for DXMS experiments. To determine the folded regions of D-AKAP2, the pepsin-cleaved peptide fragments are first identified using LC-MS/MS and Sequest software (ThermoFinnigan, Inc). Peptides representing >90% of the D-AKAP2 sequence are selected for deuterium exchange experiments. For a typical experiment, deuterated samples of D-AKAP2 are prepared by diluting 1 μl of a D-AKAP2 stock solution (50 μM) with 19 μl of deuterated buffer (10 mM HEPES, pH 7.4, 150 mM NaCl) following on-exchange incubation times of 10–3000 s. The samples are then quenched in 30 μl of 0.8% formic acid, 3.2 M GuHCl, on ice to prevent back exchange. The sample is injected into a pepsin column (66-μl bed volume, Upchurch

Scientific) up front of a C18 column that are both in line with an electrospray mass spectrometry (Micromass LC-Q), as reviewed in Woods and Hamuro (2001). Nondeuterated (ND) and fully deuterated (FD) (in 95% acidic deuterated buffer for 48 h at room temperature) control samples are processed similarly. The molecular weights of the peptide fragments are determined by measuring the centroid of the peptide isotopic envelope using Magtran software. The percentage deuteration level for each peptide is calculated as

$$\% \text{ deuteration level} = [(m(\mathrm{P}) - m(\mathrm{N}))/(m(\mathrm{F}) - m(N))] \times 100$$

where m(P), m(N), and m(F) are the centroid values of partially deuterated, nondeuterated, and fully deuterated peptides, respectively.

The percentage deuteration levels for D-AKAP2 at room temperature between 10 and 3000 s are plotted in Fig. 4. The blue colors represent regions that have a low percentage deuteration and represent regions of the protein that are either folded and/or solvent inaccessible. The red regions of the protein are areas that are more solvent accessible and/or less structured regions of the protein. The RGS domains, AKB domain, and the PDZ motif are indicated with a box. The slower exchanging regions of the protein are located in or near these domains. Sites that are susceptible to trypsin or GluC protease cleavage are indicated with arrows and map primarily within fast exchanging regions. A highly disordered region connects RGS B with the PKA-binding site. Interestingly, this region contains a consensus site for PKA phosphorylation (highlighted with an asterisk in Fig. 4) and is phosphorylated by PKA *in vitro* (data not shown). However, the structural or functional consequences of this phosphorylation are not known. If deuterium exchange data are plotted onto the modeled structure of RGS B from D-AKAP2, it is clear that the slowly exchange regions are located in the α helices and the faster exchanging regions map to the turns and loops (Fig. 2B). Exchange data support the structural model of this domain. The turn between helix 5 and 6 is the most solvent-accessible region of the RGS domain. This region in RGS4 is important for stabilizing the switch region of Gα and is implicated in enhancing GTPase activity.

The AKB domain is heavily protected from exchange in the intact protein, suggesting that this region is highly ordered in the absence of PKA (Fig. 4). In contrast, the PDZ-binding motif appears to be more disordered given the faster exchange rate for this region. This may be important for the access of interacting PDZ domains. It will be important to establish if the PKA-binding site is altered conformationally by PDZ domain binding.

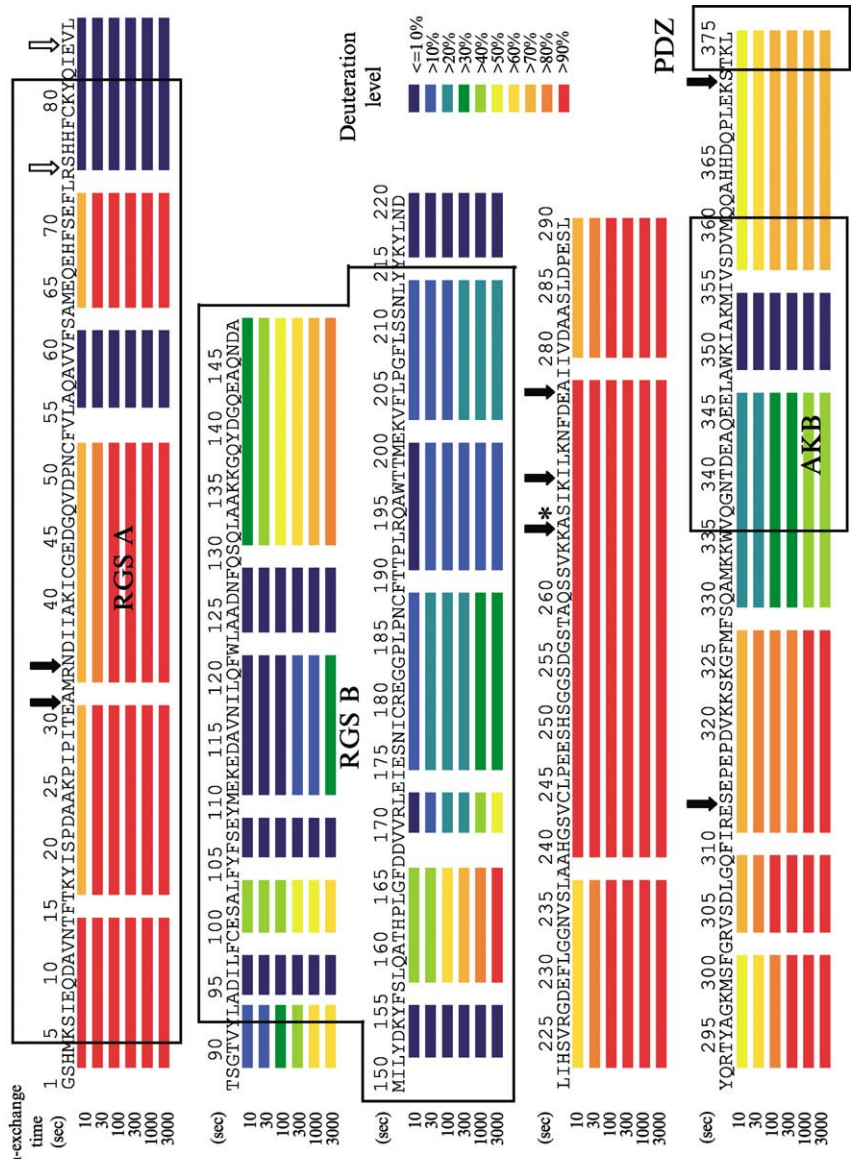
On-exchange time (sec)
RGS A
RGS B
AKB
PDZ
Deuteration level
<=10%
>10%
>20%
>30%
>40%
>50%
>60%
>70%
>80%
>90%

Designing Peptide Disruptors of AKAP-Mediated PKA Localization Using the AKB Domain of D-AKAP2

D-AKAP2 interacts with both type I and type II regulatory subunits of PKA. The regulatory subunits of PKA are not functionally redundant in the cell, which raises an interesting possibility that D-AKAP2 can tether two different types of PKA responsiveness. Type I isoforms are generally diffuse in the cytoplasm with some specific examples of cellular localization, whereas type II isoforms usually have distinct localization patterns in cells (Skalhegg and Tasken, 2000). Type I holoenzymes are also activated by lower concentrations of cAMP relative to the type II holoenzyme, suggesting that the type I enzyme can be a more sensitive trigger for cAMP-dependent kinase activation (Feliciello *et al*., 2001; Skalhegg and Tasken, 2000). The type I isoform (RIα) has been implicated in cancer (Cho-Chung *et al*., 1995), immune cell regulation (Torgersen *et al*., 2002), and the Carney complex (Casey *et al*., 2000; Kirschner *et al*., 2000), a syndrome characterized by benign tumor formation, especially in heart tissue. More recent evidence has shown that a single nucleotide polymorphism identified in human D-AKAP2 is associated with morbidity and/or mortality (as described earlier) and affects binding to only the type I isoform (RIα). These unique features attributed to RIα have prompted us to design an AKAP peptide that can bind tightly and specifically to the dimerization/docking (D/D) domain of both RIα and RIIα (Burns-Hamuro *et al*., 2003). By binding to the D/D of the regulatory subunit, the peptide can displace the localization of the holoenzyme (R_2C_2) in an isoform-dependent manner and shed light on PKA isoform-specific signaling processes.

In collaboration with Sequenom, Inc. (San Diego, CA) and Jerini AG (Berlin, Germany), we constructed peptide substitution arrays consisting of 27 amino acids from the AKB domain of D-AKAP2 to map the sequence

FIG. 4. Domain organization of D-AKAP2 probed by deuterium exchange mass spectrometry. A soluble form of mouse D-AKAP2 (372 amino acids), which included the C-terminal half of RGS A, the full RGS B domain, the PKA-binding site, and the PDZ-binding motif, was used for DXMS experiments. The deuteration level of several D-AKAP2 peptides after on exchange for 10–3000 s is presented. The peptides are denoted under the sequence of D-AKAP2 as color bars, representing the extent of deuteration (see legend). The on-exchange time is listed to the left of the sequence. Blue represents heavily protected areas, suggesting an ordered region and red represents highly exchanging regions, suggesting a disordered region. Residues corresponding to the partial RGS A domain, the full RGS B domain, the AKB domain, and the PDZ-binding motif are indicated. Limited proteolysis cleavage sites by either trypsin or Glu-C are illustrated after 1 (black arrows) and 24 (white arrows) h of digestion. The asterisk above serine 267 is highlighting an *in vitro* PKA phosphorylation site. Reprinted from Hamuro *et al.* (2002), with permission.

requirements for D-AKAP2 binding to type I and type II regulatory subunits (Burns-Hamuro *et al*., 2003). Each position in the 27 residue peptide is replaced by the other 19 L-amino acids using standard SPOT-synthesis protocols (Frank, 2002). The peptides are synthesized on an amino-functionalized cellulose membrane as distinct spots using a SPOT synthesizer with a β-alanine dipeptide spacer included between the C terminus of the peptide and the membrane support. The peptides are extended by using standard fluorenylmethoxycarbonyl (FMOC) solid-phase peptide synthesis (Wellings and Atherton, 1997), followed by cleavage of the side chain protection groups using trifluoroacetic acid (Guy and Fields, 1997). Selected peptides on the membrane are synthesized in duplicate and cleaved from the membrane using ammonia vapor in the dry state (Wenschuh *et al*., 2000) and the sequence is verified by mass spectrometry.

To screen for regulatory subunit binding to the peptide array membranes, the membranes are treated similarly to western blots. The peptide arrays are preincubated with T-TBS blocking buffer (TBS, pH 8.0/0.05% Tween 20 in the presence of a blocking reagent; Roche Diagnostics chemiluminescence detection kit 1500694). The arrays are then incubated with GFP fusion proteins of each regulatory subunit D/D domain; GFP-RIαD/D and GFP-RIIαD/D at a final concentration of 1.0 μg/ml for 2 h in T-TBS blocking buffer. After three 10-min washes, anti-GFP antibody 3E6 (Quantum Biotechnologies, Montreal) is added at 1 μg/ml for 1 h. After extensive washing, antimouse IgG peroxidase-labeled antibody (Sigma) is applied for 1 h at 1 μg/ml. Bound protein is detected using a chemiluminescence substrate and the LumiImager (Roche Diagnostics).

Results from the substitution array verified that the AKB-binding motif was α helical. There is a distinct repeating pattern of substituted residues spanning residue 12–25 that dramatically affect binding to the regulatory subunits (Fig. 5). These critical binding epitopes map to one face of an α helix. It is also apparent that the binding interaction for RII is more localized, whereas the RI interaction is dispersed over more residues (Fig. 5, highlighted by horizontal bar). Several key differences at particular substitutions are also evident (Fig. 5, circled residues). For example, substituting valine at position 21 with a tryptophan maintains binding to RI but abolishes binding to RII. The substitution arrays provided initial leads as to which substitutions could be engineered into the D-AKAP2 AKB motif to give desired isoform-selective binding.

Individual peptides are synthesized that contain single or multiple mutations that were suggested from the peptide array as having selective binding to either RI or RII. A C-terminal cysteine is engineered into each peptide during synthesis to facilitate conjugation of a fluorescent probe.

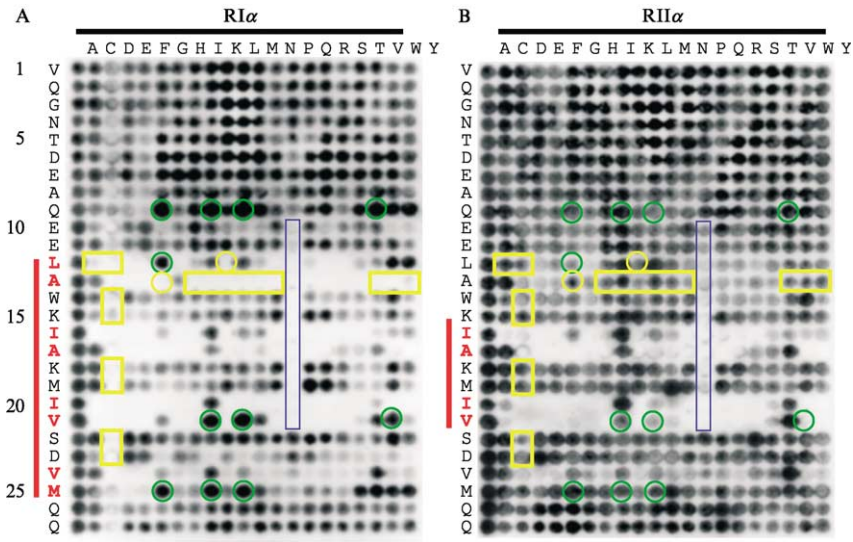

FIG. 5. A peptide substitution array of the 27 residue AKB domain of D-AKAP2 probed with either RIα (A) or RIIα (B) using an antibody sandwich detection system as described in the text. Each spot represents an immobilized peptide prepared by SPOT synthesis. All 20 amino acids (top) are substituted along each position of the AKB domain (left). Residues most sensitive to substitution are indicated in red. The bar to the left of each array highlights the region sensitive to substitution. Residues that are circled green represent peptides that show preferential binding to RIα. Residues that are boxed yellow represent peptides that show preferential binding to RIIα. Proline substitutions disrupt binding to both RI and RII along a defined sequence length (blue box). Reprinted from Burns-Hamuro *et al.* (2003), with permission.

The peptide is labeled fluorescently with tetramethylrhodamine-5-maleimide (TMRM) (Molecular Probes), which is dissolved in dimethyl sulfoxide at 25 m*M*. The peptides are labeled by incubating with a threefold molar excess of TMRM for 16 h at 4° in 20 m*M* Tris, pH 7.0, and 1 m*M* Tris-(2-carboxyethyl) phosphine, hydrochloride (TCEP) (a nonthiol-reducing agent). The labeled peptides are resolved using a reverse-phase C18 column with a water/acetonitrile gradient containing 0.1% trifluoroacetic acid. The concentration of each peptide is determined at 541 nm using the extinction coefficient for the fluorescent probe (91,000 M^{-1} cm^{-1}).

Fluorescence polarization is used to quantitate the binding of each peptide to the regulatory subunit isoforms. This technique is ideal for measuring the binding of small molecular weight species (such as peptides) to large molecular weight proteins, as the property being measured is

mobility of the labeled peptide. When the peptide becomes bound to a large protein, the mobility of the fluorophore-labeled peptide can be sufficiently reduced so as to result in a change in fluorescence polarization. This technique allows for solution determination of affinities and requires no separation of bound species. RIα and RIIα are diluted serially with either 1 or 10 n*M* of fluorescently labeled peptide in 10 m*M* HEPES, pH 7.4, 0.15 *M* NaCl, 3 m*M* EDTA, and 0.005% Surfactant P20. The samples are incubated for at least 1 h at room temperature, and fluorescence polarization is monitored using a Fluoromax-2 (JY Horiba, Edison, NJ) equipped with Glan-Thompson polarizers. The sample is excited at 541 nm (5- to 10-nm bandpass) and emission is monitored at 575 nm (5- to 10-nm bandpass). Three separate binding experiments are averaged and fit to a 1:1 binding model using the nonlinear application in GRAPHPAD PRISM version 3.00 (GraphPad, San Diego, CA). Table I summarizes the dissociation constants obtained for several of the peptides examined.

Both RI and RII selective binding peptides were designed using the peptide array approach. Experiments are underway to test whether these peptides, when added exogenously to a cell system, can selectively disrupt PKA-RI- vs PKA-RII-mediated anchoring. Preliminary evidence suggests that these peptide sequences will have the desired selectively *in vivo* as well. The peptide sequence that binds selectively to RI *in vitro* also only colocalizes with cotransfected RI and not RII as demonstrated in an artificial targeting system described previously (Burns-Hamuro *et al*., 2003). In addition, the RII selective binding peptide also colocalizes with RII and not RI using this system (Burns-Hamuro *et al*., 2003).

TABLE I
SUMMARY OF THE DISSOCIATION CONSTANTS (K_D) FOR PKA ISOFORM-SELECTIVE BINDING PEPTIDES

Peptide[a]	RIα (n*M*)	RIIα (n*M*)
WT (dual) VQGNTDEAQEELAWKIAKMIVSDVMQQ	48 ± 4	2.2 ± 0.2
AKB (PKA-RI) **F**EELAWKIAKMI**W**SDV**F**QQ	5.2 ± 0.5	456 ± 33
AKB (PKA-RII) VQGNTDEAQEEL**L**WKIAKMIVSDVMQQ	2493 ± 409	2.7 ± 0.1
AKB (PKA-Null) VQGNTDEAQEELAWKI**E**KMI**W**SDVMQQ	998 ± 66	>10,000

[a] Substituted residues are underlined in bold. Reprinted from Burns-Hamuro *et al.* (2003), with permission.

Conclusions

D-AKAP2 is an intriguing protein and evidence suggests its functional importance as an AKAP, as a PDZ-binding protein, and as a potential GPCR regulator. The implication that D-AKAP2 may be imported for recruiting PKA for vesicular trafficking and/or receptor endocytosis of kidney transporters is the first step toward identifying the functional significance of this protein. However, ubiquitous expression of D-AKAP2 in many different mouse tissues suggests that D-AKAP2 function is not restricted to the kidney. D-AKAP2 may also interact with other PDZ domains involved in organizing signaling networks at membranes. Interestingly, two additional RGS proteins, Gα interacting protein (GAIP) and RGS12 also contain PDZ-binding motifs (De Vries *et al*., 1998; Snow *et al*., 1998). GAIP has been implicated in vesicular trafficking associated with clathrin-coated vesicles and *trans*-Golgi-derived vesicles (De Vries *et al*., 1998; Wylie *et al*., 1999, 2003). Given the preliminary association with a cardiac phenotype from the SNP analysis (Kammerer *et al*., 2003), D-AKAP2 may be important for cell signaling in cardiac cells. Future work will clarify the functional role of D-AKAP2.

References

Anand, G. S., Hughes, C. A., Jones, J. M., Taylor, S. S., and Komives, E. A. (2002). Amide H/2H exchange reveals communication between the cAMP and catalytic subunit-binding sites in the RIa subunit of protein kinase A. *J. Mol. Biol.* **323,** 377–386.

Andersen, M. D., Shaffer, J., Jennings, P. A., and Adams, J. A. (2001). Structural characterization of protein kinase A as a function of nucleotide binding: Hydrogen-deuterium exchange studies using matrix-assisted laser desorption ionization-time of flight mass spectrometry detection. *J. Biol. Chem.* **276,** 14204–14211.

Bacic, D., Capuano, P., Gisler, S. M., Pribanic, S., Christensen, E. I., Biber, J., Loffing, J., Kaissling, B., Wagner, C. A., and Murer, H. (2003). Impaired PTH-induced endocytotic down-regulation of the renal type IIa Na+/Pi-cotransporter in RAP-deficient mice with reduced megalin expression. *Pflug. Arch.* **446,** 475–484.

Burns-Hamuro, L. L., Ma, Y., Kammerer, S., Reineke, U., Self, C., Cook, C., Olson, G. L., Cantor, C. R., Braun, A., and Taylor, S. S. (2003). Designing isoform-specific peptide disruptors of protein kinase A localization. *Proc. Natl. Acad. Sci. USA* **100,** 4072–4077.

Casey, M., Vaughan, C. J., He, J., Hatcher, C. J., Winter, J. M., Weremowicz, S., Montgomery, K., Kucherlapati, R., Morton, C. C., and Basson, C. T. (2000). Mutations in the protein kinase A R1alpha regulatory subunit cause familial cardiac myxomas and Carney complex. *J. Clin. Invest.* **106,** R31–R38.

Cho-Chung, Y. S., Pepe, S., Clair, T., Budillon, A., and Nesterova, M. (1995). cAMP-dependent protein kinase: Role in normal and malignant growth. *Crit. Rev. Oncol. Hematol.* **21,** 33–61.

Colledge, M., and Scott, J. D. (1999). AKAPs: From structure to function. *Trends Cell Biol.* **9,** 216–221.

De Vries, L., Lou, X., Zhao, G., Zheng, B., and Farquhar, M. G. (1998). GIPC, a PDZ domain containing protein, interacts specifically with the C terminus of RGS-GAIP. *Proc. Natl. Acad. Sci. USA* **95,** 12340–12345.

De Vries, L., Zheng, B., Fischer, T., Elenko, E., and Farquhar, M. G. (2000). The regulator of G protein signaling family. *Annu. Rev. Pharmacol. Toxicol.* **40,** 235–271.

Edwards, A. S., and Scott, J. D. (2000). A-kinase anchoring proteins: Protein kinase A and beyond. *Curr. Opin. Cell Biol.* **12,** 217–221.

Ehring, H. (1999). Hydrogen exchange/electrospray ionization mass spectrometry studies of structural features of proteins and protein/protein interactions. *Anal. Biochem.* **267,** 252–259.

Engen, J. R., Gmeiner, W. H., Smithgall, T. E., and Smith, D. L. (1999). Hydrogen exchange shows peptide binding stabilizes motions in Hck SH2. *Biochemistry* **38,** 8926–8935.

Engen, J. R., and Smith, D. L. (2001). Investigating protein structure and dynamics by hydrogen exchange MS. *Anal. Chem.* **73,** 256A–265A.

Englander, S. W., Mayne, L., Bai, Y., and Sosnick, T. R. (1997). Hydrogen exchange: The modern legacy of Linderstrom-Lang. *Prot. Sci.* **6,** 1101–1109.

Feliciello, A., Gottesman, M. E., and Avvedimento, E. V. (2001). The biological functions of A-kinase anchor proteins. *J. Mol. Biol.* **308,** 99–114.

Frank, R. (2002). The SPOT-synthesis technique: Synthetic peptide arrays on membrane supports—principles and applications. *J. Immunol. Methods* **267,** 13–26.

Gisler, S. M., Madjdpour, C., Bacic, D., Pribanic, S., Taylor, S. S., Biber, J., and Murer, H. (2003a). PDZK1. II. An anchoring site for the PKA-binding protein D-AKAP2 in renal proximal tubular cells. *Kidney Int.* **64,** 1746–1754.

Gisler, S. M., Pribanic, S., Bacic, D., Forrer, P., Gantenbein, A., Sabourin, L. A., Tsuji, A., Zhao, Z. S., Manser, E., Biber, J., and Murer, H. (2003b). PDZK1. I. A major scaffolder in brush borders of proximal tubular cells. *Kidney Int.* **64,** 1733–1745.

Gisler, S. M., Stagljar, I., Traebert, M., Bacic, D., Biber, J., and Murer, H. (2001). Interaction of the type IIa Na/Pi cotransporter with PDZ proteins. *J. Biol. Chem.* **276,** 9206–9213.

Guex, N., and Peitsch, M. C. (1997). SWISS-MODEL and the Swiss-PdbViewer: An environment for comparative protein modeling. *Electrophoresis* **18,** 2714–2723.

Guy, C. A., and Fields, G. B. (1997). Trifluoroacetic acid cleavage and deprotection of resin-bound peptides following synthesis by Fmoc chemistry. *Methods Enzymol.* **289,** 67–83.

Hamuro, Y., Burns, L., Canaves, J., Hoffman, R., Taylor, S., and Woods, V. (2002a). Domain organization of D-AKAP2 revealed by enhanced deuterium exchange-mass spectrometry (DXMS). *J. Mol. Biol.* **321,** 703.

Hamuro, Y., Burns, L. L., Canaves, J. M., Hoffman, R. C., Taylor, S. S., and Woods, V. L., Jr. (2002b). Domain organization of D-AKAP2 revealed by enhanced deuterium exchange-mass spectrometry (DXMS). *J. Mol. Biol.* **321,** 703–714.

Hamuro, Y., Coales, S. J., Southern, M. R., Nemeth-Cawley, J. F., Stranz, D. D., and Griffin, P. R. (2003). Rapid analysis of protein structure and dynamics by hydrogen/deuterium exchange mass spectrometry. *J. Biomol. Tech.* **14,** 171–182.

Hamuro, Y., Wong, L., Shaffer, J., Kim, J. S., Stranz, D. D., Jennings, P. A., Woods, V. L., Jr., and Adams, J. A. (2002c). Phosphorylation-driven motions in the COOH-terminal Src kinase, Csk, revealed through enhanced hydrogen-deuterium exchange and mass spectrometric studies (DXMS). *J. Mol. Biol.* **323,** 871–881.

Hernando, N., Deliot, N., Gisler, S. M., Lederer, E., Weinman, E. J., Biber, J., and Murer, H. (2002). PDZ-domain interactions and apical expression of type IIa Na/P(i) cotransporters. *Proc. Natl. Acad. Sci. USA* **99,** 11957–11962.

Hoofnagle, A. N., Resing, K. A., and Ahn, N. G. (2003). Protein analysis by hydrogen exchange mass spectrometry. *Annu. Rev. Biophys. Biomol. Struct.* **32,** 1–25.

Huang, L. J., Durick, K., Weiner, J. A., Chun, J., and Taylor, S. S. (1997a). D-AKAP2, a novel protein kinase A anchoring protein with a putative RGS domain. *Proc. Natl. Acad. Sci. USA* **94,** 11184–11189.

Huang, L. J., Durick, K., Weiner, J. A., Chun, J., and Taylor, S. S. (1997b). Identification of a novel protein kinase A anchoring protein that binds both type I and type II regulatory subunits. *J. Biol. Chem.* **272,** 8057–8064.

Huang, L. J., Wang, L., Ma, Y., Durick, K., Perkins, G., Deerinck, T. J., Ellisman, M. H., and Taylor, S. S. (1999). NH_2-terminal targeting motifs direct dual specificity A-kinase-anchoring protein 1 (D-AKAP1) to either mitochondria or endoplasmic reticulum. *J. Cell Biol.* **145,** 951–959.

Kammerer, S., Burns-Hamuro, L. L., Ma, Y., Hamon, S. C., Canaves, J. M., Shi, M. M., Nelson, M. R., Sing, C. F., Cantor, C. R., Taylor, S. S., and Braun, A. (2003). Amino acid variant in the kinase binding domain of dual-specific A kinase-anchoring protein 2: A disease susceptibility polymorphism. *Proc. Natl. Acad. Sci. USA* **100,** 4066–4071.

Kirschner, L. S., Carney, J. A., Pack, S. D., Taymans, S. E., Giatzakis, C., Cho, Y. S., Cho-Chung, Y. S., and Stratakis, C. A. (2000). Mutations of the gene encoding the protein kinase A type I-alpha regulatory subunit in patients with the Carney complex. *Nature Genet.* **26,** 89–92.

Ma, Y., and Taylor, S. (2002). A 15-residue bifunctional element in D-AKAP1 is required for both endoplasmic reticulum and mitochondrial targeting. *J. Biol. Chem.* **277,** 27328–27336.

Mandell, J. G., Baerga-Ortiz, A., Akashi, S., Takio, K., and Komives, E. A. (2001). Solvent accessibility of the thrombin-thrombomodulin interface. *J. Mol. Biol.* **306,** 575–589.

Murer, H., Hernando, N., Forsten, I., and Biber, J. (2003). Regulation of Na/Pi transporter in the proximal tubule. *Annu. Rev. Physiol.* **65,** 531–542.

Okazaki, Y., Furuno, M., Kasukawa, T., Adachi, J., Bono, H., Kondo, S., Nikaido, I., Osato, N., Saito, R., Suzuki, H., Yamanaka, I., Kiyosawa, H., Yagi, K., Tomaru, Y., Hasegawa, Y., Nogami, A., Schonbach, C., Gojobori, T., Baldarelli, R., Hill, D. P., Bult, C., Hume, D. A., Quackenbush, J., Schriml, L. M., Kanapin, A., Matsuda, H., Batalov, S., Beisel, K. W., Blake, J. A., Bradt, D., Brusic, V., Chothia, C., Corbani, L. E., Cousins, S., Dalla, E., Dragani, T. A., Fletcher, C. F., Forrest, A., Frazer, K. S., Gaasterland, T., Gariboldi, M., Gissi, C., Godzik, A., Gough, J., Grimmond, S., Gustincich, S., Hirokawa, N., Jackson, I. J., Jarvis, E. D., Kanai, A., Kawaji, H., Kawasawa, Y., Kedzierski, R. M., King, B. L., Konagaya, A., Kurochkin, I. V., Lee, Y., Lenhard, B., Lyons, P. A., Maglott, D. R., Maltais, L., Marchionni, L., McKenzie, L., Miki, H., Nagashima, T., Numata, K., Okido, T., Pavan, W. J., Pertea, G., Pesole, G., Petrovsky, N., Pillai, R., Pontius, J. U., Qi, D., Ramachandran, S., Ravasi, T., Reed, J. C., Reed, D. J., Reid, J., Ring, B. Z., Ringwald, M., Sandelin, A., Schneider, C., Semple, C. A., Setou, M., Shimada, K., Sultana, R., Takenaka, Y., Taylor, M. S., Teasdale, R. D., Tomita, M., Verardo, R., Wagner, L., Wahlestedt, C., Wang, Y., Watanabe, Y., Wells, C., Wilming, L. G., Wynshaw-Boris, A., Yanagisawa, M. *et al.* (2002). Analysis of the mouse transcriptome based on functional annotation of 60,770 full-length cDNAs. *Nature* **420,** 563–573.

Perkins, G. A., Wang, L., Huang, L. J., Humphries, K., Yao, V. J., Martone, M., Deerinck, T. J., Barraclough, D. M., Violin, J. D., Smith, D., Newton, A., Scott, J. D., Taylor, S. S., and Ellisman, M. H. (2001). PKA, PKC, and AKAP localization in and around the neuromuscular junction. *BMC Neurosci.* **2,** 17.

Resing, K. A., Hoofnagle, A. N., and Ahn, N. G. (1999). Modeling deuterium exchange behavior of ERK2 using pepsin mapping to probe secondary structure. *J. Am. Soc. Mass Spectrom.* **10,** 685–702.

Skalhegg, B. S., and Tasken, K. (2000). Specificity in the cAMP/PKA signaling pathway. Differential expression, regulation, and subcellular localization of subunits of PKA. *Front. Biosci.* **5,** D678–D693.

Snow, B. E., Hall, R. A., Krumins, A. M., Brothers, G. M., Bouchard, D., Brothers, C. A., Chung, S., Mangion, J., Gilman, A. G., Lefkowitz, R. J., and Siderovski, D. P. (1998). GTPase activating specificity of RGS12 and binding specificity of an alternatively spliced PDZ (PSD-95/Dlg/ZO-1) domain. *J. Biol. Chem.* **273,** 17749–17755.

Tesmer, J. J., Berman, D. M., Gilman, A. G., and Sprang, S. R. (1997). Structure of RGS4 bound to AlF4-activated G(i alpha1): Stabilization of the transition state for GTP hydrolysis. *Cell* **89,** 251–261.

Torgersen, K. M., Vang, T., Abrahamsen, H., Yaqub, S., and Tasken, K. (2002). Molecular mechanisms for protein kinase A-mediated modulation of immune function. *Cell Signal.* **14,** 1–9.

Wang, L., Sunahara, R. K., Krumins, A., Perkins, G., Crochiere, M. L., Mackey, M., Bell, S., Ellisman, M. H., and Taylor, S. S. (2001). Cloning and mitochondrial localization of full-length D-AKAP2, a protein kinase A anchoring protein. *Proc. Natl. Acad. Sci. USA* **98,** 3220–3225.

Weinman, E. J., Steplock, D., Donowitz, M., and Shenolikar, S. (2000). NHERF associations with sodium-hydrogen exchanger isoform 3 (NHE3) and ezrin are essential for cAMP-mediated phosphorylation and inhibition of NHE3. *Biochemistry* **39,** 6123–6129.

Weinman, E. J., Steplock, D., and Shenolikar, S. (2001). Acute regulation of NHE3 by protein kinase A requires a multiprotein signal complex. *Kidney Int.* **60,** 450–454.

Wellings, D. A., and Atherton, E. (1997). Standard Fmoc protocols. *Methods Enzymol.* **289,** 44–67.

Wenschuh, H., Volkmer-Engert, R., Schmidt, M., Schulz, M., Schneider-Mergener, J., and Reineke, U. (2000). Coherent membrane supports for parallel microsynthesis and screening of bioactive peptides. *Biopolymers* **55,** 188–206.

Woods, V. L., and Hamuro, Y. (2001). High resolution, high-throughput amide deuterium exchange-mass spectrometry (DXMS) determination of protein binding site structure and dynamics: Utility in pharmaceutical design. *J. Cell. Biochem.* **S37,** 89–98.

Wylie, F., Heimann, K., Le, T. L., Brown, D., Rabnott, G., and Stow, J. L. (1999). GAIP, a Galphai-3-binding protein, is associated with Golgi-derived vesicles and protein trafficking. *Am. J. Physiol.* **276,** C497–C506.

Wylie, F. G., Lock, J. G., Jamriska, L., Khromykh, T., L., Brown, D., and Stow, J. L. (2003). GAIP participates in budding of membrane carriers at the trans-Golgi network. *Traffic* **4,** 175–189.

Yan, X., Zhang, H., Watson, J., Schimerlik, M. I., and Deinzer, M. L. (2002). Hydrogen/deuterium exchange and mass spectrometric analysis of a protein containing multiple disulfide bonds: Solution structure of recombinant macrophage colony stimulating factor-beta (rhM-CSFb). *Pro. Sci.* **11,** 2113–2124.

Zhang, Z., and Smith, D. L. (1993). Determination of amide hydrogen exchange by mass spectrometry: A new tool for protein structure elucidation. *Prot. Sci.* **2,** 522–531.

Zheng, B., De Vries, L., and Gist-Farquhar, M. (1999). Divergence of RGS proteins: Evidence for the existence of six mammalian RGS subfamilies. *Trends Biochem. Sci.* **24,** 411–414.